Wind-Induced Ventilation

F. Allard M. Herrlin

ABSTRACT

Wind-induced ventilation is studied analytically in a simple one-zone structure and numerically in a three-zone building. The paper focuses on the wind effect, but because wind influence cannot be treated independently of other main driving forces, the wind effect is studied with and without stack effect and mechanical exhaust.

The analytical part describes the basic equations that are necessary to predict ventilation rates. These equations are applied to a simple structure to make it possible to study the principal meaning and influence of each one of the parameters in an analytical way. The magnitude and importance of each parameter are discussed.

The numerical part shows an actual calculation of a multi-zone structure. The infiltration for each zone is shown as a function of wind effect alone and in combination with stack effect and mechanical exhaust. This demonstrates the non-trivial interaction between the different driving forces.

INTRODUCTION

Airflows around buildings can significantly modify infiltration and ventilation control and, consequently, the indoor climate, contaminant control, energy consumption, and even equipment operation. To be able to predict the influence of wind on a building is obviously a necessary task.

Until now, various methods and numerical models have been developed to estimate infiltration and ventilation rates. Liddament and Allen (1983) made a short review and more recent models have been developed by Walton (1984), Roldan (1985), and Clarke (1985).

These various models are based upon a representation of the building by a network of nodes representing the pressures of rooms or zones. The connections between these nodes are described by nonlinear equations giving the flows as functions of the pressure differences. Conservation of air mass inside each zone leads to a system of nonlinear equations that has to be solved iteratively.

Despite this apparent complexity, these phenomena can be described easily, and then estimates can be made using the elements of handbooks like chapters 14 and 22 of the ASHRAE Fundamentals (ASHRAE 1985, 1989).

This paper will emphasize the influence of wind effect on infiltration rates and its couplings with stack effect due to buoyancy, and a mechanical exhaust system.

At first, a simple case is presented of a single-zone building where the calculation can be made analytically. With this elementary example, the influence of wind, stack effect, and mechanical exhaust on infiltration can easily be discussed.

Then, in a more realistic approach, the case of a multizone building is described. The influences of wind and pressure coefficients, stack effect, and mechanical exhaust on infiltration rates are presented and discussed using numerical means. The infiltration and ventilation simulation program MOVECOMP is used for these calculations (Herrlin 1988).

PHYSICAL BACKGROUND

Bernouilli's Equation

For steady, incompressible, and nonviscous flow, the Navier-Stokes equation can be integrated and reduced to a simpler expression, combining the transport effect due to velocity, pressure effect, and gravity effect upon a field of density.

$$1/2\ \rho V^2 + P + \rho\ g\ z = Cste \qquad (1)$$

Equation 1, combining the local values of pressure, velocity, and density fields, is known as Bernouilli's equation. It is the fundamental equation necessary to understand and predict the behavior of airflows in a building submitted to the combined influence of a natural environment (wind, outdoor temperature, pressure, and humidity) and an indoor climate (temperature, mechanical ventilation, and humidity). The next step is to define precisely the effects of all these internal and external climatic parameters.

Wind Effect and Pressure Coefficients

The driving forces for natural ventilation are the pressure and velocity fields induced by wind around a building together with the stack effect.

When a flow hits an obstacle, its velocity creates an instantaneous overpressure. The dynamic pressure, P_{dyn}, due to the flow is given by Bernouilli's equation:

$$P_{dyn} = 1/2\ \rho\ V^2 \qquad (2)$$

In Equation 2 V represents the instantaneous local wind velocity at upwind position of the obstacle.

To use such an instantaneous equation is not possible in the case of buildings, since the wind velocity varies too much in space and time. So the pressures generally used are time-averaged values with an averaging period of about 10 minutes. Instantaneous pressures may vary

F. Allard is Charge de Recherche CNRS, Centre de Thermique de L'INSA de Lyon, France; **M. Herrlin** is Staff Scientist, Division of Building Services Engineering, Royal Institute of Technology, Sweden.

significantly above and below these averages, and peak values two or three times the mean values are not uncommon. While the knowledge of peak values is important with regard to structural load calculations, the mean values are more appropriate for computation of infiltration and ventilation rates. Since the mean values also obey Bernouilli's equation, we can write,

$$P_V = 1/2\ \rho\ V_H^2 \tag{3}$$

In Equation 3, V_H represents the mean wind velocity at upwind building height and ρ the outdoor air density as a function of atmospherical pressure, temperature, and humidity.

This local wind velocity can be estimated by applying terrain and height corrections to the velocity given by a nearby meteorological station.

The pressure difference, P_S, between the pressure on the building envelope and atmospherical pressure is obtained by correcting the pressure, P_V, given by the undisturbed flow by an empirical coefficient, C_P.

$$P_S = C_P\ P_V \tag{4}$$

Values of the pressure coefficient C_P depend mainly on the building shape, wind direction, and influence of nearby buildings and natural environment. Accurate determination of C_P can only be obtained from wind tunnel tests of a model of the specific building and site. However, reasonable estimates of infiltration and ventilation rates can be predicted using existing wind tunnel data.

Chapter 14 of ASHRAE Fundamentals (ASHRAE 1989) gives various examples of C_P distribution on buildings (see Figures 5 and 6). More information about C_P values can be found in Gandemer (1978), Bowen (1976), and Swami (1987).

Stack Effect

Another physical phenomenon that influences the infiltration and ventilation rates in buildings is the effect of buoyancy, or stack effect. This is due to density differences between inside and outside air or between two zones of a building. The density is mainly a function of temperature and moisture content of air.

In Figure 1, Z_N represents the reference altitude of zone N, whose reference pressure, temperature, and humidity are P_N, T_N, and H_N. Z_J represents the local altitude of the leakage in zone N. With the same conventions, we obtain, in zone M, $Z_$ for the relative altitude of the leakage, Z_M for the reference altitude of zone M, P_M for its reference pressure, T_M for its reference temperature, and H_M for its reference relative humidity.

The driving pressure difference is given by the local pressure difference between the two sides of the leakage ($P_I - P_J$). However, it is more convenient to write it relative to the reference pressures of each zone,

$$P_{I} - P_{J} = P_{I_0} - P_{J_0} + P_{S} \tag{5}$$

In Equation 5 P_S represents the stack effect

$$P_S = \rho_M\ g\ (Z_{I_0} - Z_I) - \rho_N\ g\ (Z_{J_0} - Z_J) \tag{6}$$

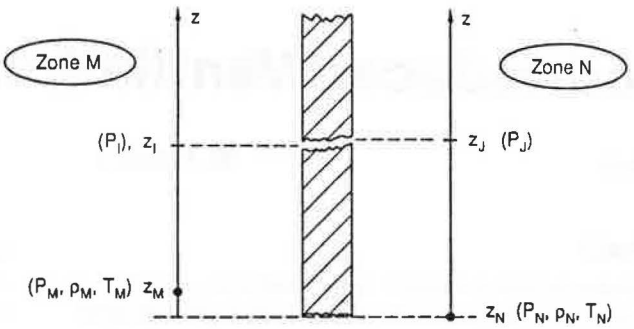

Figure 1 *Stack effect*

In Equation 6 ρ_M and ρ_N represent the values of the air density in each zone due to temperature and moisture content of air.

Flow Equations

With Bernouilli's equation we can get a theoretical expression of the velocity of a flow due to a pressure difference. The theoretical mass flow rate, m_t', of a fluid with a density ρ through an opening of area A would be:

$$m_t' = \rho\ A \sqrt{\frac{2\ \Delta P}{\rho}} \tag{7}$$

In fact, the flow is affected by the geometrical characteristics of the opening. For simple geometrical configurations, it is possible to define a discharge coefficient C_d relating the real mass flow, m', to the theoretical one:

$$m' = C_d\ \rho\ A \sqrt{\frac{2\ \Delta P}{\rho}} \tag{8}$$

Furthermore, it appears that for leakages of complex structures, the dependency of the pressure difference is even more complicated. Therefore, an empirical power law function is usually used:

$$m' = K_1\ \bar{\rho}\ \bar{2}\ A_e\ \Delta P^n \tag{9}$$

In Equation 9, the exponent of the flow equation, n, varies theoretically between 0.5 for a fully developed turbulent flow and 1 for a laminar one. A_e represents a free area equivalent to the real crack. But in most practical problems, it is not possible to get a precise description of each leak; then a general law can be defined as:

$$m' = K\ \Delta P^n \tag{10}$$

K and n represent the general characteristics of a leakage. The value of the flow coefficient K can be interpreted as the value of the flow rate induced by a unitary pressure difference.

Mass Conservation Equation

Under assumed static conditions, the conservation of mass inside each elementary control volume has to be ensured. In building ventilation studies, this control volume, called a zone, can be a room or any group of rooms that are assumed to have the same pressure level.

For each leak, the mass flow rate can be evaluated using Equation 10. The instantaneous mass balance of air

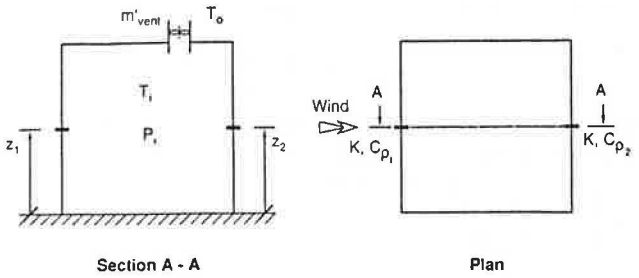

Figure 2 *General definition of the studied case*

inside any zone is obtained assuming that the sum of all the flows is equal to zero. If the zone under consideration includes a mechanical exhaust system, this system can be represented by the expression of the extracted flow, m'_{vent}. A general form of the balance equation in each zone of a building would be:

$$m'_{vent} + \sum_{k=1}^{k=N} m'_k = 0 \qquad (11)$$

N represents the number of distinct leakage areas in the zone, and m'_k represents the mass flow rate through leakage area k.

CASE STUDY 1

A simple example is developed to show how the different physical laws defined above can be used to estimate the infiltration rates in a building. The building to be considered here is a single-zone structure with only two leakage areas located on its two opposite facades. Figure 2 gives a general view of the geometry.

Combined Influences of the Wind Velocity and Flow Equation Coefficients *K* and *n*

In this first study, we assume that neither temperature differences nor humidity variations between indoor and outdoor climate exist. Consequently, the only phenomenon affecting the natural ventilation of this building is the wind.

The pressure differences due to wind effect on each facade are defined by Equation 4 and the expressions of the pressures due to wind effect upon each facade can then be written as,

$$P_1 = 1/2\ C_{P1}\ \rho\ V^2$$

and (12)

$$P_2 = 1/2\ C_{P2}\ \rho\ V^2$$

The values of the average coefficients C_{P1} and C_{P2} can be taken from Chapter 14 of ASHRAE Fundamentals. If we assume P_i to be the reference pressure of the indoor climate, we will obtain the following pressure differences between both sides of each facade.

$$\Delta P_1 = P_1 - P_i$$

and (13)

$$\Delta P_2 = P_2 - P_i$$

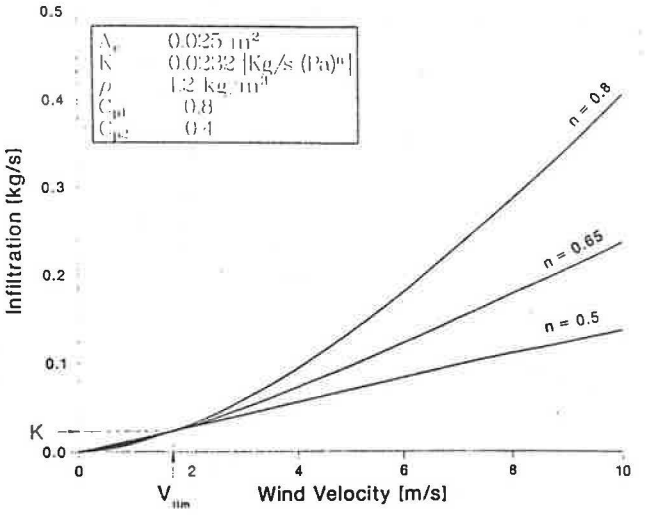

Figure 3 *Infiltration rate as a function of wind velocity for different values of the exponent n*

The incoming mass airflow rate through each facade may be defined using Equation 10, and can be obtained with $\Delta P_1 > 0$ and $\Delta P_2 < 0$:

$$m'_1 = K_1\ \Delta P_1^n$$

and

$$m'_2 = -K_2\ |\ \Delta P_2\ |^n$$

The flow coefficient K can be determined by a blower door experiment or calculated by defining the equivalent leakage area of each wall. Chapter 22 of ASHRAE Fundamentals (ASHRAE 1985) defines simplified estimates of leakage areas in buildings using Tables 2 through 14.

The mass conservation for the air inside the building can be expressed as,

$$m'_1 + m'_2 = 0$$

Since we assumed that the two leakage areas located in each facade are identical, we get:

$$\Delta P_1 + \Delta P_2 = 0$$

The internal pressure reference P_i and the infiltration rate m' can now be defined,

$$P_i = \frac{\rho V^2}{4}\left(C_{P1} + C_{P2}\right) \qquad (14)$$

and

$$m' = K\left[\frac{\rho V^2}{4}\left(C_{P1} - C_{P2}\right)\right]^n \qquad (15)$$

Looking at Equation 15, we can see clearly that the flow rate is directly proportional to the flow coefficient K, whereas the dependency upon the exponent of the flow equation is much more difficult to define. It depends in fact on the pressure difference.

For high values of the pressure difference, i.e.

$$\left|\frac{\rho V^2}{4}\left(C_{P1} - C_{P2}\right)\right| > 1,$$

the flow rate increases if the flow remains laminar ($n - 1$).

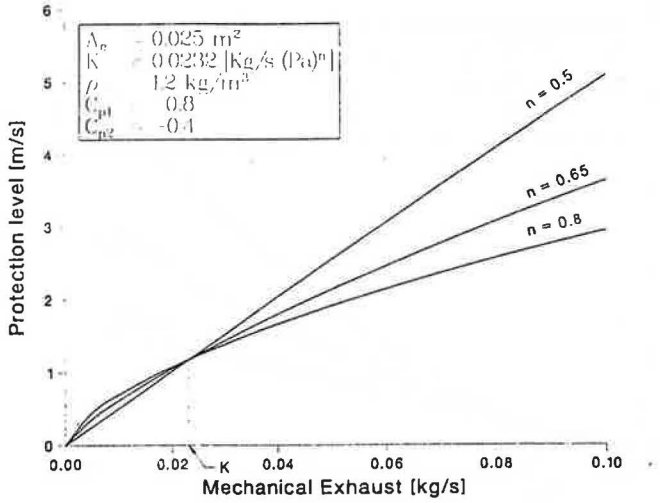

Figure 4 *Protection level given by an exhaust ventilation system as a function of its flow rate*

For pressure differences below this value, the opposite behavior is obtained—the flow rate decreases when the flow is turbulent ($n-.5$).

This behavior is shown in Figure 3, which shows the infiltration rate as a function of the wind velocity for three values of the exponent n. The intersection between the three curves represents a unitary pressure difference. The abscissa gives the corresponding wind velocity, the ordinate represents the flow coefficient K.

Coupling with an Exhaust System

If we assume m'_{vent} to be the mass flow of air extracted by a mechanical exhaust system, the mass balance equation becomes,

$$m'_1 + m'_2 = m'_{vent} \tag{16}$$

We can define the protection level of our exhaust system as the maximum wind velocity it can accept without producing a crossflow through the building. This is equivalent to the wind velocity, $V_{p'}$, which cancels the pressure difference across the downwind facade. Below this level ($\Delta P_2 > 0$), all the exhaust air passes through the ventilation system.

Using Equations 12 and 13 it is easy to determine the resulting internal pressure, P_i,

$$\Delta P_2 = 0 \longrightarrow P_i = 1/2\ \rho\ V_{p'}^2\ C_{P2}$$

Then the infiltration rate through the upwind facade is:

$$m'_1 = K\left[1/2\ \rho\ V_{pl}^2 C_{P1} - 1/2\ \rho\ V_{pl}^2 C_{P2}\right]^n$$

This flow equals m'_{vent} and the protection level of our exhaust system can be defined as,

$$V_{p'} = \left[\frac{m'_{vent}}{K}\right]^{1/2n} \sqrt{\frac{2}{\rho(C_{P1} - C_{P2})}} \tag{17}$$

Figure 4 shows the calculation of this protection level with the exhaust ventilation rate m'_{vent} for three different values of the flow equation exponent n. The intersection point of the three curves corresponds to equal magnitudes for m'_{vent} and K. Above this point, the protection level decreases when the flow becomes laminar ($n-1$), while below this point the protection level increases when the flow is laminar.

Coupling with Stack Effect

We are now considering a building without an exhaust system but with a temperature difference between indoor and outdoor climates. We assume an indoor temperature of 20°C and an outdoor temperature of 0°C. Three configurations for the leakage location on each facade will now be studied. Figure 5 presents these three cases.

Using Equations 5 and 6, it is easy to define the new values of the pressure differences across the two facades,

$$\Delta P_1 = 1/2\ \rho_0\ C_{P1} V^2 - P_i - Z_1\ (\rho_0 - \rho_{20})$$

and (18)

$$\Delta P_2 = 1/2\ \rho_0\ C_{P2} V^2 - P_i - Z_2\ (\rho_0 - \rho_{20})$$

Assuming that the flow coefficient K and the exponent n of the flow equation (Equation 10) do not change with temperature, the internal pressure reference becomes,

$$P_i = \frac{\rho_0 V^2}{4}(C_{P1} + C_{P2}) - \frac{Z_1 + Z_2}{2}(\rho_0 - \rho_{20})$$

Figure 6 shows the evolution of the incoming flow through facade 1 for the three configurations, when the wind velocity varies from 0 to 10 m/s.

In configuration 1, the stack effect does not change the incoming flow. The internal pressure, P_i, is modified by the stack effect, but the pressure difference across each facade is not affected.

In configuration 2, the stack effect reduces the internal pressure too, but it increases the pressure difference across both facades. The pressure difference across

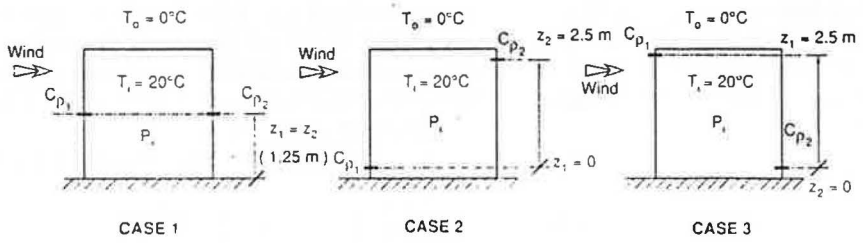

Figure 5 *Sketch of the three configurations studied*

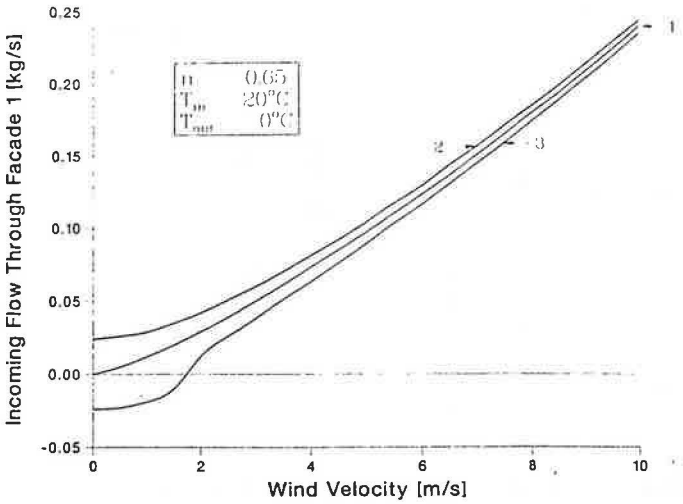

Figure 6 *Calculation of the incoming flow through the upwind facade*

facade 1 depends only on the altitude of the leakage area on facade 2 and on the temperature of indoor and outdoor climates:

$$\Delta P_1 = 1/4\rho_0 V^2 \left[C_{P1} - C_{P2}\right] + \frac{Z_2 g(\rho_0 - \rho_{20})}{2}$$

As shown in Figure 6, the result is a general increase in the infiltration through facade 1. For low wind velocities, this increase is very significant (50% at 2 m/s).

In configuration 3, the incoming flow through facade 1 starts negative, because the stack effect creates a reversed pressure difference across facade 1.

$$\Delta P_1 = 1/4\,\rho_0 V^2 \left[C_{P1} - C_{P2}\right] - \frac{Z_1 g(\rho_0 - \rho_{20})}{2}$$

Until the wind effect balances this value, the air is outgoing through facade 1. This limit is given by the general expression of ΔP_1, which leads to:

$$V_{lim} = \sqrt{\frac{2Z_1 g(\rho_0 - \rho_{20})}{\rho_0(C_{P1} - C_{P2})}} \qquad (19)$$

CASE STUDY 2

As has been shown in the preceding section, the influence of different parameters and the interpretation of results for a single-zone structure are quite straightforward.

The scope of this second case study is to show the complex interaction between building characteristics and driving forces in a multi-zone building. The results, which are not as predictable as one may expect, will be discussed in an informal way.

The calculations are carried out with a detailed multizone infiltration model (Herrlin 1987) because an analytical approach is not practical or even possible.

Building Description

The building under consideration is a three-zone, two-story structure with an interconnecting staircase (see Figure 7).

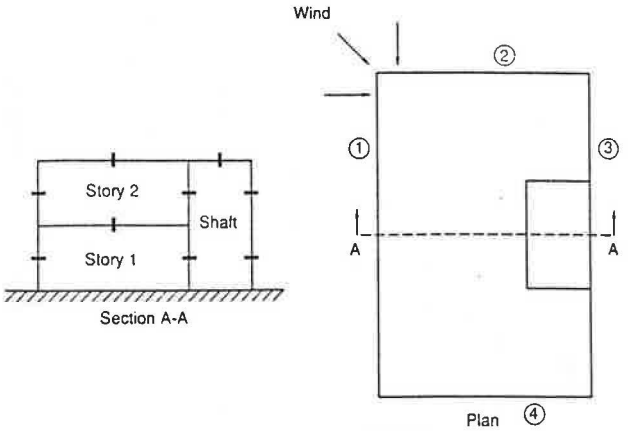

Figure 7 *Layout of building*

Each story has a 90 m² area with a room height of 2.4 m, and 10 m² of staircase. The overall leakage is equivalent to 9 air changes per hour at 50 Pa pressure difference between the inside and outside. This leakage level is at the lower end for U.S. residential buildings and corresponds to an air change rate of 0.6 at a wind velocity of 4 m/s. The exponent in the flow equation (Equation 10) is set to 0.65, which is a common value for entire buildings. The leakage is assumed to be evenly distributed over the shell of the building, including the roof. Also, the internal separations have the same leakage rate per area. This assumption has mainly been done to simplify the understanding of the following calculations and results.

Influence of Wind Velocity and Wind Direction on Infiltration

The infiltration will first be studied when the building is exposed to various wind velocities from three different directions. The Cp-values (Equation 4) have been determined from Figure 6, Chapter 14, of ASHRAE Fundamentals (ASHRAE 1989). This figure is relevant for low-rise buildings, defined as $h < w$, where h is the height and w is the width of the building perpendicular to the wind. The Cp-values used for the calculation are given in Table 1.

The results are shown in Figure 8. The air change rates are calculated with reference to the total building volume.

The differences of the infiltration rates are approximately within ±15% throughout all wind velocities. It may be somewhat surprising that the infiltration resulting from a wind hitting the building at a 45° angle is the largest. This is due to the fact that this is the only case where two outer surfaces contribute to the infiltration. Another reason is the highly nonlinear form of the flow equations. This gives rise

TABLE 1
C_p-Values for Each Wall

Cp	1	2	3	4	Roof
90	.75	-.45	-.45	-.45	-.50
45	.35	.30	-.45	-.30	-.50
0	-.30	.70	-.30	-.15	-.50

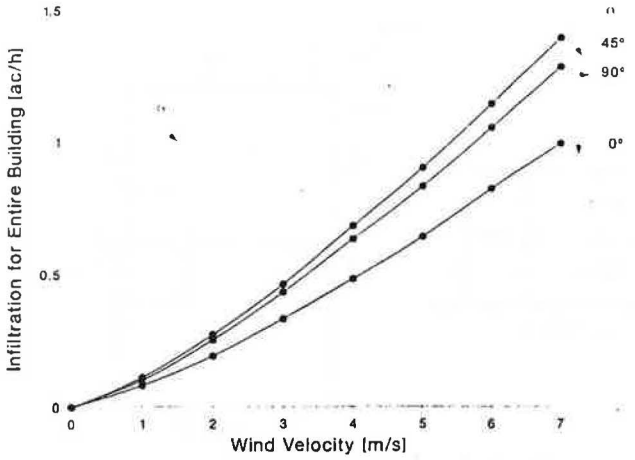

Figure 8 *Infiltration as a function of wind velocity with wind direction as parameter*

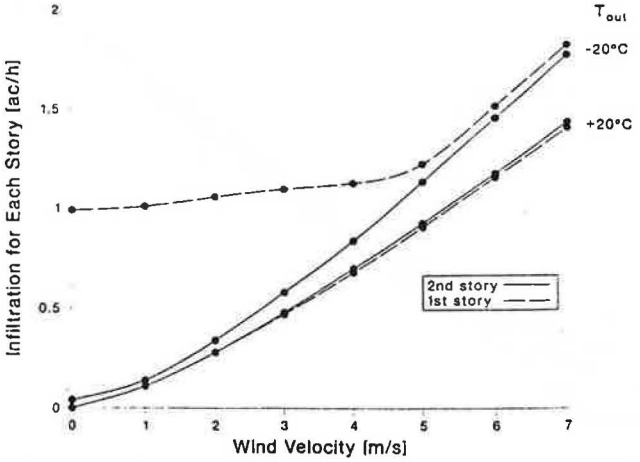

Figure 9 *Infiltration as a function of wind velocity with stack effect as parameter*

to a lower pressure loss, i.e., a higher flow rate, despite the lower driving force across the building compared to the case when the wind hits the building at a 90° angle.

Influence of Wind Velocity and Stack Effect on Infiltration

The infiltration rates are now studied independently for each story and with the assumption that the wind strikes the building at a 90° angle.

The influence of wind velocity only is presented first. The two lower curves in Figure 9 represent the two stories at an outer temperature of 20°C, which is equal to the indoor temperature. As can be seen, the curves are almost identical. These curves are the same as the curve in Figure 8 for the same wind direction with the only difference that we now calculate the infiltration rate with reference to the volume of each story.

The infiltration rate is slightly larger on the second story because of the negative outer pressure of the roof and its important leakage area. The large area of the slab compared to the windward wall makes the difference small.

Stack effect is now added to the wind effect according to Equation 6. The outer temperature is lowered to −20°C, increasing the stack effect.

The infiltration rate for the first story at lower wind velocities is almost constant and equal to the stack effect. At higher wind velocities, on the other hand, the infiltration rate is almost determined by the wind effect only. We have two quite well separated regions, one determined by the stack effect and one by the wind forces.

The infiltration rate for the second story does have the same behavior, although it is not obvious looking at the figure. The stack effect is too small here compared to the wind effect to be apparent in the figure.

The big difference in levels at zero wind depends on the flow through the shaft that increases the infiltration rate in the first story and decreases it in the second story. If the roof had been tighter, we would have seen no infiltration at all in the second story.

Both curves at −20°C are steeper than the curves at 20°C due to the higher air density and consequently higher dynamic pressures of the wind.

Influence of Wind Velocity, Stack Effect, and Mechanical Exhaust on Infiltration

As was demonstrated in the previous section, the infiltration rates can become inadequate at low wind velocities and small temperature differences between the inside and outside of the building. To eliminate this disadvantage, we introduce mechanical exhaust, which ensures a minimal ventilation.

The exhaust flow rate for each story is set to 110 m^3/h, which is equivalent to 0.5 air changes per hour. This does not necessarily mean that all this air originates as infiltration in the same zone.

Figure 10 shows the infiltration rates at the same outdoor temperatures as before, i.e., 20°C and −20°C. As we saw in the previous section, the stack effect did not change the infiltration on the second floor very much. It is therefore expected that at lower wind velocities, the difference between the infiltration rates for these temperatures with fan forces present is small and is determined primarily by the exhaust only.

At 20°C, i.e., with no stack effect present, the curves are fast approaching the curves in Figure 9 at higher wind velocities. The fan force is thus a second order effect. At lower wind velocities, the second story has a larger infiltration due to the leakage area of the roof. The infiltration of the first story is lower than 0.5 air changes per hour at low wind velocities because a part of the air extracted by the exhaust fan originates from the second story and the shaft. The flow through the roof changes direction to exfiltration at higher wind velocities, which creates the dip in the curve for the second story.

At −20°C the curves are approaching the curves in Figure 9 but at a higher wind velocity compared with 20°C. Above this velocity, both the thermal and fan forces are of second order. The first story has a very high infiltration rate over the whole range of wind velocities. The thermal and fan forces work here in the same direction. The second story has, as expected, an infiltration rate close to the rate at 20°C. The stack effects increase the wall infiltration, but, more importantly, they will change the roof infiltration to exfiltration. The dips in the curves again are due to changes in flow directions.

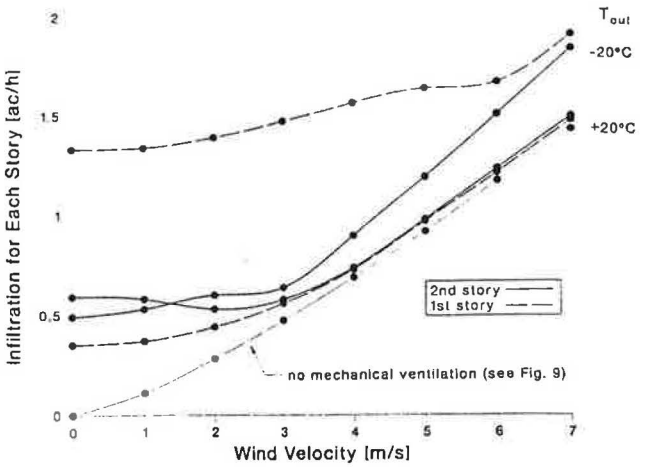

Figure 10 *Infiltration as a function of wind velocity with stack effect and mechanical exhaust as parameters*

CONCLUSION

Very simple structures can be examined analytically with data from one of many handbooks. The benefit with this approach is that the results and general influence or meaning of the different parameters that are involved can be evaluated without interference of the complexity of larger structures. In the first case study, we developed single expressions showing that the infiltration rate and protection level are strongly dependent on the flow coefficient and exponent. In the same way, the interaction between stack effect and wind regarding infiltration rate was demonstrated. The results are easy to understand and serve therefore as a good introduction to airflow problems.

Larger structures require systematic investigation with a powerful tool such as a multi-zone infiltration model. The interpretation of infiltration calculations requires extensive insight into the problem, even when the building is relatively small as in the second case study. For large buildings, it is virtually impossible to understand the results if the calculations are not planned very carefully. Even so, the results from larger structures with many zones do not necessarily give any general understanding of the complex interaction between building characteristics and driving forces.

This case study also shows clearly the variations of air change rates due to outer conditions. The wind and the stack effect seem to play an equally important role here. The only way to make the air change rates of our building less dependent on natural driving forces is to build tighter structures, to design exhaust systems with a sufficient protection level, or to control both supply and exhaust of air.

NOMENCLATURE

A = area of leak, m^2
Ae = equivalent area, m^2
Cp = pressure coefficient
g = gravity, m/s^{-2}
K = flow coefficient, $kg/s^{-1}\ Pa^{n}$
m' = mass flow rate, kg/s^{-1}
n = flow exponent
P = pressure, Pa
V = velocity, m/s^{-1}
z = altitude, m
ρ = air density, kg/m^{-3}

REFERENCES

ASHRAE. 1985. *ASHRAE handbook—1985 fundamentals*, chapter 22. Atlanta: American Society of Heating, Refrigerating, and Air-Conditioning Engineers, Inc.

ASHRAE. 1989. *ASHRAE handbook—1989 fundamentals*, chapter 14. Atlanta: American Society of Heating, Refrigerating, and Air-Conditioning Engineers, Inc.

Bowen, A.J. 1976. "A wind tunnel investigation using simple building models to obtain mean surface wind pressure coefficients for air infiltration estimates." National Council of Canada Technical Report LTR-LA 209, p. 108.

Clarke, J.A. 1985. *Energy analysis in building design*. Bristol and Boston: Adam Hilger Ltd.

Gandemer, J. 1978. "Champ de pression moyenne sur les constructions usuelles. Application a la conception des installations de ventilation." *Cahiers du Centre Scientifique et Technique du Batiment*, No. 197, p. 35.

Herrlin, M.K. 1987. "Luftstromning i byggnader—en berakningsmodell." Licentiate Thesis, Division of Building Services Engineering, Royal Institute of Technology, Stockholm, Sweden, p. 125.

Herrlin, M.K. 1988. "MOVECOMP—a multizone infiltration and ventilation simulation program." *Air Infiltration Review*, Vol. 9, No. 3.

Liddament, M., and Allen, C. 1983. "The validation and comparison of mathematical models of air infiltration." Air Infiltration Center Technical Note AIC 11, September, p. 113.

Roldan, A. 1985. "Etudes thermiques et aerauliques des envelopes de batiment: influence des couplages interieurs et du multizonage." Doctoral thesis, National Institute of Applied Sciences, Lyon, France, p. 310.

Swami, M.V., and Chandra, S. 1987. "Procedure for calculating natural ventilation airflow rates in buildings." Florida Solar Energy Center, ASHRAE Research Project 448-RP. Final Report FSCCR-163-86, p. 120.

Walton, G.N. 1984. "A computer algorithm for predicting infiltration and interroom airflows." *ASHRAE Transactions*, Vol. 90, Part 1.